Desalination and Water Treatment
www.deswater.com

doi: 10.5004/dwt.2019.23328

138 (2019) 80–90
January

Preparation and characterization of high-flux poly(*m*-phenylene isophthalamide) (PMIA) hollow fiber ultrafiltration membrane

Qinliang Jiang[a,b], Kaisong Zhang[a,*]

[a]*Key Laboratory of Urban Pollutant Conversion, Institute of Urban Environment, Chinese Academy of Sciences, Xiamen 361021, China*
[b]*University of Chinese Academy of Sciences, Beijing 10049, China, emails: kszhang@iue.ac.cn (K. Zhang), qljiang@iue.ac.cn (Q. Jiang)*

Received 28 May 2018; Accepted 20 October 2018

ABSTRACT

The tradeoff between membrane flux and rejection remains the most challenging issues confronting membrane application in water industry. In this work, a poly(*m*-phenylene isophthalamide) (PMIA) hollow fiber ultrafiltration membrane with corresponding high flux and rejection of bovine serum albumin was successfully fabricated by phase inversion technique. Further, we systematically investigated the effects of PMIA content, LiCl and PEG400 concentrations, respectively, on the morphologies and separation performance of PMIA hollow fiber ultrafiltration (UF) membranes. Results reveal that the water flux of hollow fiber membrane decreased with the increase of PMIA content while the rejection of BSA increased. Compared with the membranes prepared without PEG as an additive, formation of dense sponge-like structures favored higher hydrophilicities for membranes with PEG additive. And the results showed that membrane under optimized conditions (LiCl 4wt%, PEG 2wt%) exhibited an increased pure water flux (239.63 L m^{-2} h^{-1}) and higher rejection rate of BSA (98.50%) under the operation pressure of 0.1 Mpa. Considering their maximum stress (4 MPa) and good BSA solution flux, the hollow fiber UF membranes are believed to have great potential for application in wastewater filtration.

Keywords: Hollow fiber; Ultrafiltration; Poly(*m*-phenylene isophthalamine); Additives; High flux

1. Introduction

The water crisis is one of the most important issues in modern society which promote many water treatment technologies. Among all the techniques, membrane filtration, especially ultrafiltration owing to its several advantages (such as flexibility, cost effectiveness, efficiency, environment friendliness), has become the most attractive and successfully applied in diverse water treatment applications such as wastewater treatment, water purification, protein concentration and enzyme extraction [1–3]. Currently, various polymeric materials with the advantages of good membrane forming ability and low cost have been widely used in the preparation of hollow fiber UF membrane, such as polysulfone, polyethersulfone, poly(vinylidene fluoride) (PVDF), and polyvinyl chloride [4–8]. Nowadays, most commercial UF membranes are made from these above polymers, which makes the membrane susceptible to organic fouling, especially in some special applications, such as bio-separation, membrane bioreactor (MBR), etc [9–12]. One of the approaches to fix this obstacle is to endow the membrane surface with the hydrophilicity which can promote the water diffusion, slow the irreversible adsorption of biological pollutants on membrane surface. The research of hydrophilic polymer as new membrane materials is attracting more and more attention.

Poly(*m*-phenylene isophthalamide) (PMIA) has become one of the most important structural materials for membrane fabrication because of its hydrogen bond network, which leads to excellent mechanical properties and outstanding thermal stability (Tg = 558 K) [13]. Meanwhile,

* Corresponding author.

the hydrophilicity of PMIA is due to the large number of amide bonds in the polymer backbone which endows the PMIA membrane with excellent wettability and can improve the water permeation and resist fouling in ultrafiltration process. Additionally, it is easy to prepare PMIA membrane by non-solvent induced phase separation (NIPS) owing to its dissolvability in two common organic solvents (such as DMF and DMAC), which is favorable for developing large-scale UF membranes [14].

In the last decade, PMIA has attracted so much attention as the promising membrane materials because of its comprehensive properties, especially its excellent separation property. NIPS is a simple and convenient technique for the fabrication of UF membranes. PMIA asymmetric membranes are mainly prepared by dry/wet phase inversion method. To achieve a desired membrane morphology and performance, the phase inversion process must be completely controlled [15–17]. Several reports utilized the traditional NIPS method for the fabrication of PMIA flat sheet and hollow fiber NF membrane membranes [18,19]. Wang et al. [19] successfully prepared PMIA hollow fiber NF membrane and discussed the effects of the type and the concentration of additives in the dope solution on membrane performance. Huang and Zhang [18] prepared flat-sheet PMIA nanofiltration membranes and studied some factors, such as organic non-solvent additives, curing treatment time and temperature, on the membrane performance. Chen et al. [20] used flat-sheet PMIA ultrafiltration membrane as the support of the thin film composite (TFC) membranes by interfacial polymerization and investigated the effects of the properties of substrates on performance and thermal stability of TFC membrane. Other researchers also reported modification studies beside the above mentioned, such as a report about PMIA with organically modified montmorillonite to improve the hydrophilicity and the ionic character [21]. In order to prepare a desired polymer with thermal stability, hydrophilicity and fouling resistance, Yang et al. [22] incorporate GO into the PMIA NF membrane and the results demonstrate that the membrane water flux, rejections to several certain dyes and antifouling property were enhanced.

Up to now, almost all researches on PMIA used to fabricate high performance membranes material mainly focus on the preparation of flat-sheet ultrafiltration and nanofiltration membrane. However, to the best of the authors' knowledge, there are no reports about fabricating PMIA hollow fiber ultrafiltration membranes by dry/wet spinning technique yet. Although PMIA flat-sheet UF membranes had already been successfully fabricated, the PMIA hollow fiber membrane has not since the formation mechanism and controlling factors for hollow fiber membrane by phase inversion is much more complicated than its flat-sheet counterpart [23]. The asymmetric structure of hollow fiber membranes prepared by the immersion precipitation process have been widely applied in separation process because of its intrinsic advantages (such as high packing density, ease of module fabrication and low operation cost) compared with flat-sheet ones [24–27]. Additionally, the improved hollow fiber substrate properties have been proven to improve the performance of some TFC membranes [28]. Due to the lack of study of PMIA hollow fiber NF membrane, it is worth enough to investigate the effects of PMIA hollow fiber support on the performance of TFC NF membranes.

The primary objective of this study is to explore suitable spinning parameters for developing PMIA hollow fiber UF membrane. The effects of PMIA content, the type and the concentration of non-solvent additives on the morphology and the performance of hollow fiber ultrafiltration membranes were studied extensively. Finally, the mechanical properties and BSA solution flux of the prepared PMIA hollow fiber ultrafiltration membranes in this work were also investigated.

2. Experimental setup

2.1. Materials

Commercial PMIA was purchased from DuPont Co,. Ltd. (United States). Its chemical structure is shown in Fig. 1. LiCl, PEG (Mw = 400) were supplied by Sinopharm Chemical Reagent Co., Ltd. N,N-dimethylacetamine (DMAC, >99%) was purchased from Shanghai Jingwei Chemical Co., Ltd. Bovine serum albumin (BSA, Mw = 67,000) and humic acid (HA) were acquired from Sigma-Aldrich (Germany).

2.2. Membrane preparation

The polymer was dried at 105°C for 12 h before use. The dope solution was prepared by dissolving predetermined amounts of PMIA, solvent and additives in a flask in proper order and mechanically stirred at 70°C for at least 12 h to guarantee complete dissolution of the polymer. After that, the polymer solution was kept in a 5 L reaction tank (50°C, 24 h) for vacuum degasification. Table 1 lists the compositions of all dope solutions.

Dry-wet phase inversion process [26] was adopted to prepare the hollow fiber membrane. The polymer solution was coextruded by a bore fluid with a precise syringe pump equipped to control the dope flow rate. Tap water was used as an external coagulant. The scheme of the spinning apparatus used to fabricate the PMIA hollow fiber UF membrane in this work is shown in Fig. 2.

The nascent fiber would pass through a line of air gap, coagulant bath and roller which was used to collect the produced samples with a fixed take up speed. The detailed spinning parameters are summarized in Table 2. All the nascent hollow fibers were rinsed in a circulating DI water bath for at least 48 h to remove the residual solvent and additives and stored in a 50wt% glycerol aqueous solution for 48 h prior to air drying at room temperature.

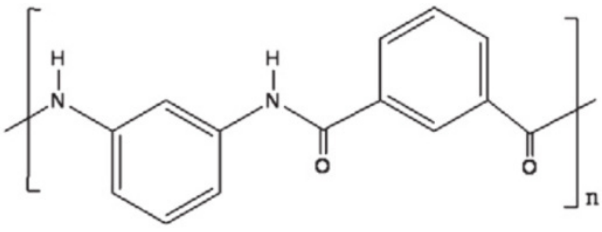

Fig. 1. Chemical structure of PMIA.

Table 1
Spinning parameters for samples M1-M13

Membrane code	PMIA (wt%)	LiCl (wt%)	PEG400 (wt%)	DMAC (wt%)	Viscosity (cp)
M1	12	4	0	84	7,560 ± 35
M2	14	4	0	82	8,940 ± 43
M3	16	4	0	80	10,620 ± 37
M4	18	4	0	78	34,800 ± 54
M5	14	3	0	83	5,790 ± 37
M6	14	3.5	0	82.5	6,870 ± 44
M7	14	4.5	0	81.5	8,310 ± 26
M8	14	5	0	81	12,990 ± 43
M9	14	4	1	81	10,209 ± 48
M10	14	4	2	80	10,470 ± 56
M11	14	4	3	79	10,770 ± 60
M12	14	4	4	78	11,010 ± 54
M13	14	4	5	77	12,230 ± 61

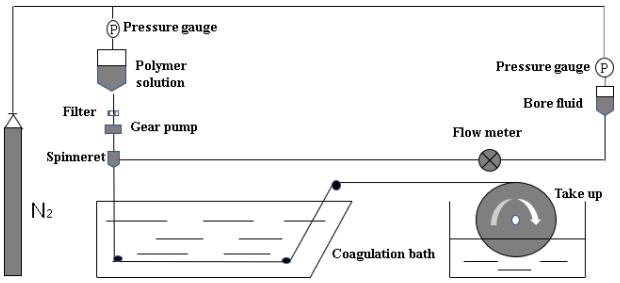

Fig. 2. Schematic diagram of the spinning apparatus for PMIA hollow fiber membrane.

Table 2
Preparation parameters and spinning conditions of hollow fiber membrane

Preparation parameters/spinning conditions	Value
Dope solution temperature (°C)	50
Spinneret dimension OD/ID (mm/mm)	1.6/0.9
Dope solution flow rate (mL/min)	5.75
Bore solution flow rate (mL/min)	4.75
Bore solution	Deionized water
External coagulation	Tap water
Coagulation temperature (°C)	25 ± 1
Air gap distance (cm)	10
Take up speed	Free fall

2.3. Characterization of membrane

2.3.1. Morphology of the membrane

Surface and cross-section morphologies of the prepared PMIA hollow fiber membranes ware studied using a field emission scanning electron microscope (FESEM) (HITACHI S4800, Hitachi. Ltd., Japan). And liquid nitrogen was used to fracture the cross section of the hollow fiber. The mounted membrane was sputtered with gold nanoparticle under vacuum using a HITACHI E-1010 ion sputtering coater.

2.3.2. Pore sizes and distribution

The membrane surface pore sizes and distribution under wet state were measured by the membrane pore analyzer (PSMA-10, XuH Science and Technology Co. Ltd., China) based on liquid/liquid displacement porosimetry [29].

2.3.3. Viscosity and porosity

The viscosity of the casting solution was determined using a numerical display viscometer (LVDC-C, Brookfield, USA). The measurements were carried out at 25°C with spindle of S64.

The membrane porosity ε (%) was defined as the volume of the pores divided by total volume of the porous membrane. It could be calculated with 10 mL specific gravity bottle by a gravimetric method [30]:

$$\varepsilon(\%) = \frac{(W1 - W2)/\rho_w}{(W1 - W2)/\rho_w + (W2/\rho_p)} \times 100\% \quad (1)$$

where W_1 is the weight of wet membrane (g), W_2 is the weight of dry membrane (g), ρ_w and ρ_p are the densities of the water and polymer, respectively. All the samples for each membrane were tested five times and the average value was reported.

2.3.4. Membrane contact angle

The hydrophilicity of PMIA hollow fiber membranes was evaluated by a contact angle analyzer (KRUSS DSA30, Germany). At least 20 water contact angles at different locations on membrane surface were averaged and reported.

2.3.5. Filtration performance

Hollow fiber membrane modules were self-prepared (outside feeding), two hollow fibers with effective length of 50 cm were composed into a module, the permeate solutions exited from the fiber lumen side. The pure water permeability of PMIA hollow fiber membrane was measured by a cross-flow ultrafiltration experiments after the pre-pressured process at 1.5 bar with deionized water for 30 min. All experiments were conducted at 25°C ± 1°C with a feed pressure of 1.0 bar. Then the permeation properties of PMIA hollow fiber membranes were characterized by the rejection BSA aqueous solution. The concentrations of permeate and feed solution were determined by an ultraviolet spectrophotometer (UV3600 Shimadzu, Japan). The permeation flux (J) and rejection (R) was measured by the following equations (Eqs. (1) and (2)), respectively [31].

$$J_w = \frac{Q}{A \cdot t} \quad (2)$$

$$R = \left(1 - \frac{C_p}{C_f}\right) \quad (3)$$

where J was the permeation flux of membrane for pure water ($L \cdot m^{-2} \cdot h^{-1}$), Q was the volume of the membrane permeate pure water (L), A was the membrane area (m^2) and t was the ultrafiltration time (h). R was the solute rejection, C_f was the feed concentration (mg/L), C_p was the permeate concentration (mg/L).

2.3.6. Measurement of mechanical properties

Mechanical properties of membranes were measured using tensile testing equipment (AGX-10KN). The samples were stretched at an elongation rate of 10 mm/min at room temperature (25°C) and at relative humidity of 50%. The fiber was initially fixed by grips at distance of 50 mm, after which the movable crosshead containing the load cell of 1 KN pulled the fiber at a constant rate of 10 mm/min until the fiber was broken. Three samples were selected randomly and tested from each batch of the dried hollow fiber.

2.3.7. BSA solution flux

In order to investigate the fouling resistance of the membrane, BSA was used as a model foulant. BSA concentration in the feed solutions was 1.0 g L^{-1}. The experiments were performed according to the following steps. The PMIA membranes were compacted at 2.0 bar for 30 min. Then BSA solution was filtered through the membrane at 1.0 bar for 2 h and the flux of the foulant solution was measured.

3. Results and discussion

3.1. Viscosity

The viscosity of polymer solution is an important factor in the formation of the membrane which can influence kinetics of the phase inversion, the phase separation speed and the gelation dynamics and ultimately affect the morphology and structure of the membrane [32].

Therefore, the viscosity of PMIA/LiCl/DMAC casting solution was measured as a function of different polymer solutions. The results are shown in Table 1. It can be seen that viscosity of the dope solution is proportional to the polymer concentration in which the viscosity of the solution increases from 7,560 to 34,800 cp with the increase of polymer content from 12 to 18wt%. This can be attributed to the size of polymer network which was increased by enhancing the interaction between the polymer molecules at the cost of the interaction between polymer and solvent. It indicates that the strength of interaction between polymer and solvent molecule is slightly greater than that of polymer molecules. The increasing size of polymer network on account of polymer chain interpenetration increases the viscosity of the polymer solution [33].

As the concentration of LiCl increases from 3 to 5wt%, the dope viscosities increase from 5,970 to 12,990 cp. This is because of the complex formation between the carbonyl group of DMAC and LiCl via ion-dipole interaction [34]. Table 1 shows that compared with the viscosity of dope solution M2, the introduction of PEG further increases the dope viscosity. The reason is that the higher affinity between the PEG and DMAC molecules which reduces the dissolving power of DMAC and enhances the PMIA molecule interaction. In this situation, the composition of polymer dope is closer to the precipitation point, the polymer chains may have more tightly coiled conformation and form aggregations which enhances the viscosity of the casting solution [35].

3.2. Effects of polymer content

Polymer content in dope is one of the most crucial factors affecting the ultimate morphology and performance of membrane. Therefore, dope solution with different PMIA content (12–18wt%) have been formulated to investigate their effects on the characteristics of hollow fiber UF membranes. The SEM photographs (cross section; inner edge; outer edge; external surface) of membranes spun at different PMIA contents are shown in Fig. 3. As it can be observed that structure (M1-CS/OE/IE) with an outer layer finger-like voids and inter layer large macrovoids was formed in the cross section of hollow fiber membrane with 12 and 14wt% PMIA in the casting solution, respectively. With further increase of PMIA content in the polymer solution, it can be seen in Fig. 3 that the inter layer large macrovoids decrease both in size and number, which are replaced by a sponge-like structure inner layer when the PMIA content increases to 18wt%. This is due to the higher viscosity of PMIA casting solution which will slow down the diffusion of non-solvent into the membrane which in turn decreases the exchange speed between solvent solution and water. It indicates that higher PMIA content in casting solution tends to suppress the formation of large macrovoids. It is in good agreement with the findings of Prince et al. [36] that macrovoids and cavity structures were formed when exchange rate is fast and sponge-like structures are formed when the exchange rate is low.

Effects of polymer content on the performance of PMIA UF membranes are shown in Fig. 4. The BSA rejection increased from 90.60% to 98.50% of hollow fiber UF membranes with increasing PMIA content in casting solution from 12 to 18wt% while pure water flux decreased from 333.55 to 66.48 L m^{-2} h^{-1}. These variations can be rationalized by the overall membrane porosity and pore size in the external surface which is one of the main factors to determine the performance of the membranes. The morphologies of membranes cross sections changed from loose large macrovoid structure into dense sponge structure when the polymer content increases. The dense sponge structure would reduce the overall porosity and pore size of the membrane (Table 3), it can be seen from Fig. 3 (M1-ES to M4-ES) that with higher PMIA concentration, the structures of external surface show the change from one with a discrete pore distribution of appreciable dimensions to almost compact surface layer. As a result, the pure water flux decreased and the rejection rate of the PMIA membranes increased. To get the desired rejection of BSA without obviously sacrificing pure water flux, the PMIA content was fixed at 14wt% for further study.

3.3. Effects of LiCl concentration

Another key factor that determined the phase-inversion rate of a membrane forming system is the concentration of

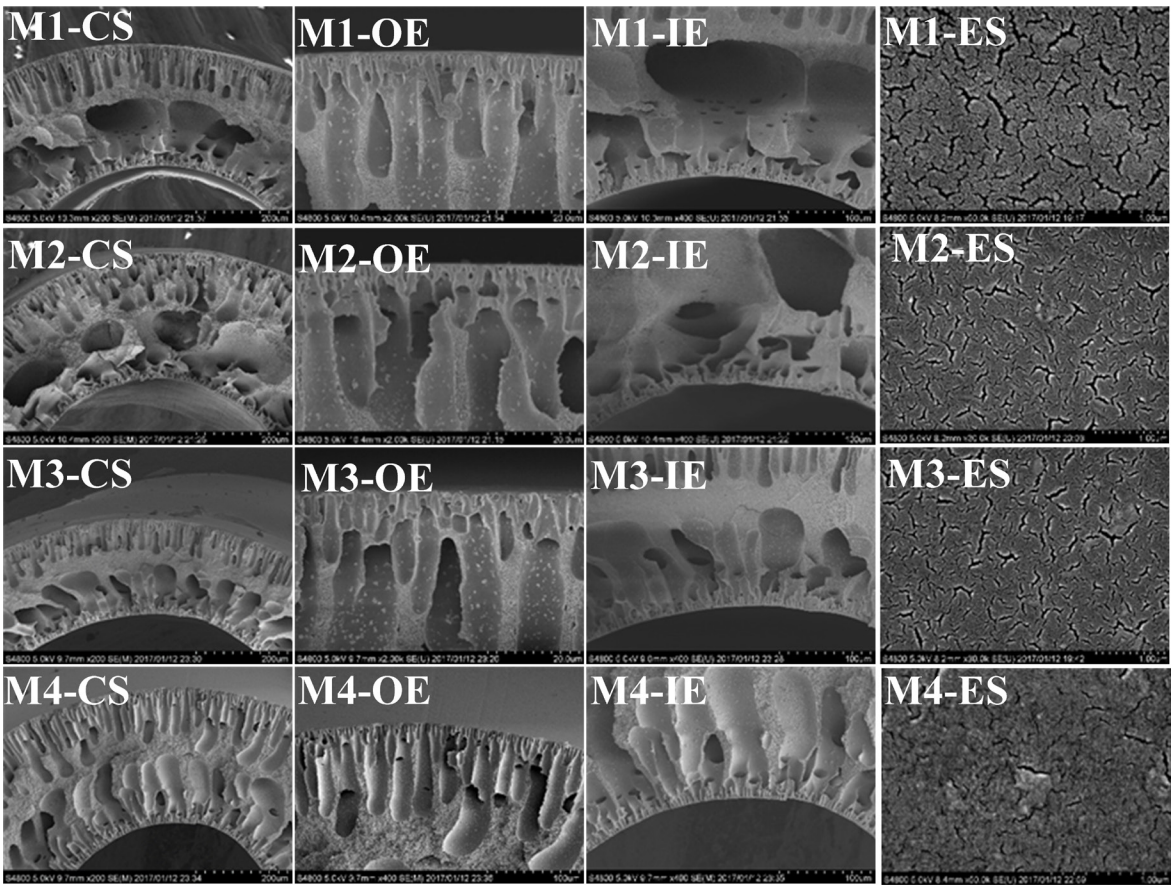

Fig. 3. Effect of different PMIA content in the polymer solution on the morphologies (CS: cross section; IE: inner edge; OE: outer edge; ES: external surface) of the hollow fiber membranes.

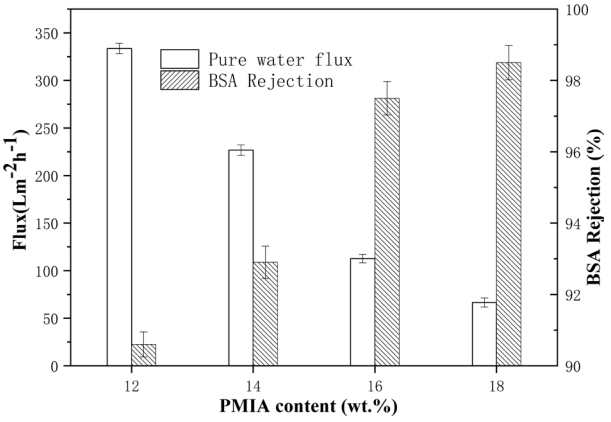

Fig. 4. Effect of PMIA content on the performance of hollow fiber UF membranes.

pore-forming agent in casting solution. Usually, the addition of inorganic molecular additive in casting solution contributes to change the phase separation rate. Fig. 5 shows that the membrane morphologies of the cross section, the inner/outer layer and the external surface of PMIA hollow fiber ultrafiltration membranes with different LiCl concentration. It can be seen from Fig. 5 that the PMIA hollow fiber membrane M5 (LiCl 3wt%) and M6 (LiCl 3.5wt%) have similar

Table 3
Effect of PMIA content on the characteristic of the membrane

Sample	OD (nm)	ID (nm)	δ/mm	Porosity (%)	Mean pore size (nm)
M1	1.069	0.644	0.2125	84.84	130.34
M2	1.221	0.713	0.254	81.62	8.965
M3	1.326	0.774	0.276	80.42	8.194
M4	1.348	0.810	0.269	77.07	6.6

OD, outer diameter, ID, inner diameter, δ, wall thickness.

structures, exhibiting inner layer large voids and outer layer finger-like extended to the middle of cross section where a sponge-like structure at the middle of cross section. While membrane M2-CS (Fig. 3) with 4wt% LiCl concentration shows that finger-like structure become even larger and the number of pores also increases. Furthermore, the external surface structure of the PMIA hollow fiber membrane M5 prepared with 3wt% LiCl in the dope solution looks more density, while membrane M7 looks more porous. The experimental results illustrate that the precipitation of PMIA forming the membrane external surfaces and the exchange of solvents with non-solvents may be affected by the diffusion of the water-soluble additives LiCl from the dope solution to the water bath. Besides, there are more and large cracks

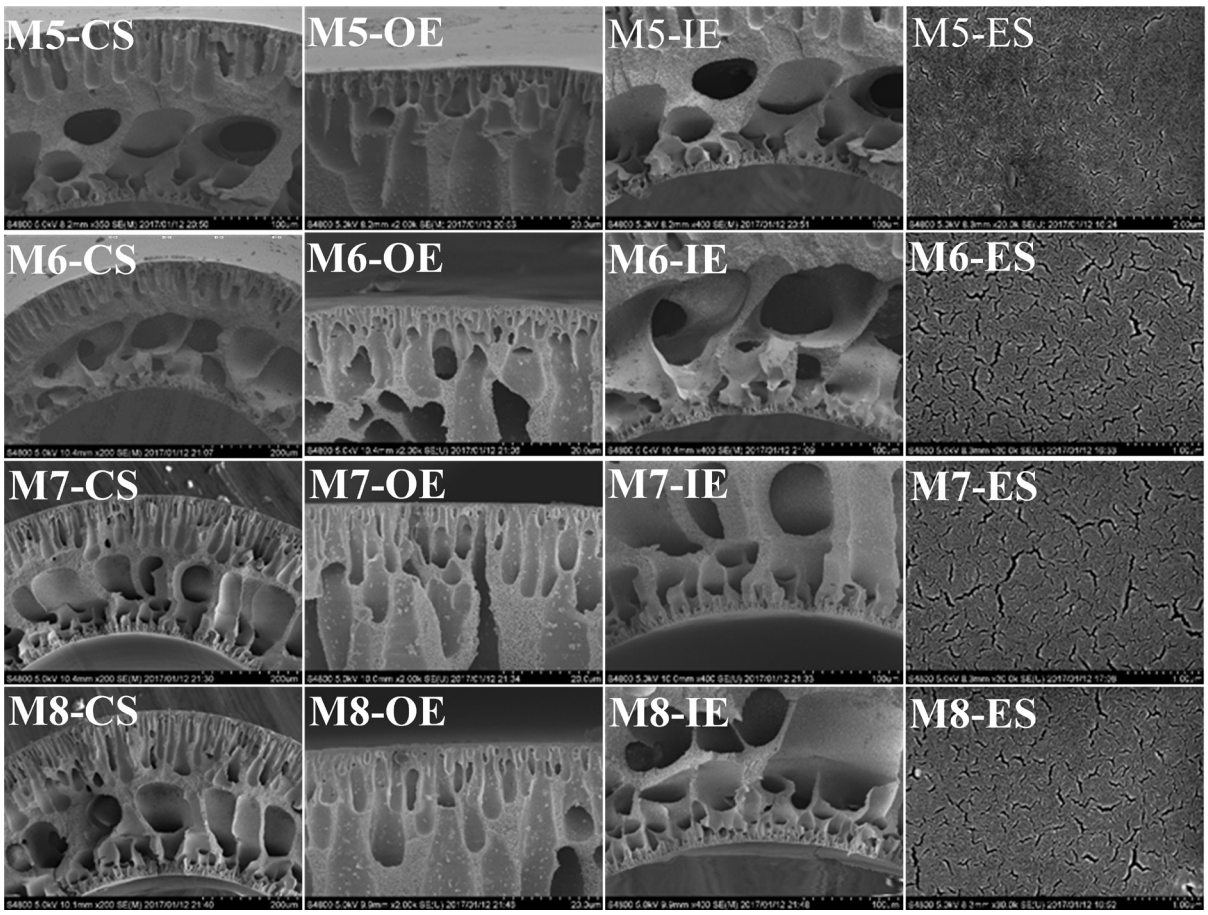

Fig. 5. Effect of LiCl concentration in the polymer solution on the morphologies (CS: cross section; IE: inner edge; OE: outer edge; ES: external surface) of the hollow fiber membranes.

in membrane M7 with 4wt% LiCl whereas few cracks can be found on the membrane surface of membrane M5. This result demonstrated that the addition of LiCl decreased the thermodynamic stability of the polymer solution and facilitate the diffusion of water and the formation of larger macrovoids. Additionally, the mutual complexation between Li ions and electron donor groups of PMIA could reduce the interaction between the polymer molecules. However, when more LiCl is added into the dope solution, the number and size of finger-like macrovoids slightly decreased due to the drastic increase of the viscosities of the casting solution through adding LiCl (Table 1). Higher viscosity tends to reduce the phase inversion rate and delay the dope precipitation [37]. As a result, Fig. 5 shows that the macrovoids of inner layer become longer and narrower and the size and number of finger-like structure close to the outer layer reduced when the content of LiCl is more than 4wt%.

Effect of LiCl concentration on the performance of hollow fiber UF membranes was studied and the results are shown in Fig. 6. According to Fig. 6, the water flux of the UF membrane increased from 114.19 to 226.85 L m^{-2} h^{-1} when the LiCl concentration increased from 3 to 4wt%. Moreover, rejection of BSA solution decreased from 94.74% to 92.90%. It might be due to increased membrane pore size and porosity with the addition of LiCl (Table 4). Additionally, the inorganic

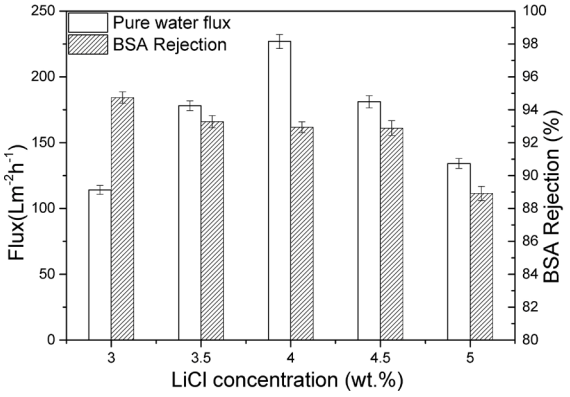

Fig. 6. Effect of LiCl concentration on the performance of hollow fiber UF membranes.

salt may be leached out from the polymer matrix when the membrane is immersed into a coagulation bath, which contributed to the formation of microporous membrane and hence the enhancement of water flux. However, further addition of LiCl additive more than 4wt% could reduce the phase inversion rate since increasing the viscosity of polymer solution took in charge and it retarded the formation process of UF membranes, which resulted in a dense sponge-like

top surface layer. Therefore, it decreased the water flux and increased rejection of BSA.

3.4. Effect of PEG concentration

With an attempt to suppress the macrovoids formation, the different concentration of PEG was used as organic additive in the dope solution to make a comparative study compared with inorganic LiCl additive. The cross-sectional SEM images of the resultant membranes fabricated with different PEG content are shown in Fig. 7.

Table 4
Effect of LiCl concentration on the characteristic of the membrane

Sample	OD (nm)	ID (nm)	δ (mm)	Porosity (%)	Mean pore size (nm)
M5	1.272	0.763	0.2545	79.64	10.648
M6	1.319	0.72	0.2995	81.85	8.855
M7	1.272	0.669	0.305	82.24	8.924
M8	1.312	0.763	0.2745	81.79	10.126

OD, outer diameter, ID, inner diameter, δ, wall thickness.

It can be seen from Fig. 7 that all the resultant membranes show a typical asymmetrical structure of a thin dense top-layer and a porous sub-layer with droplet morphologies near the inner edge. Compared with the membranes prepared with and without PEG as the additive (Fig. 3 M2, Fig. 7), the presence of PEG favored the formation of dense sponge-like structure, which was confirmed from the cross-section morphology near inner layer and outer layer. Between the macrovoids beneath the outer layer and above the inner layer of the membranes were suppressed to some extent, the cross-section morphology of all the membranes was altered to the sponge-like structure compared with the membrane M2 (Fig. 3). PMIA membrane with PEG additive did not show more macrovoid (Fig. 7). Because PEG can increase the viscosity of the polymer solution (Table 1), higher PEG concentration would hinder the exchange rate of solvent and non-solvent and lead to a denser structure in the membrane. Additionally, another possible explanation could be that a

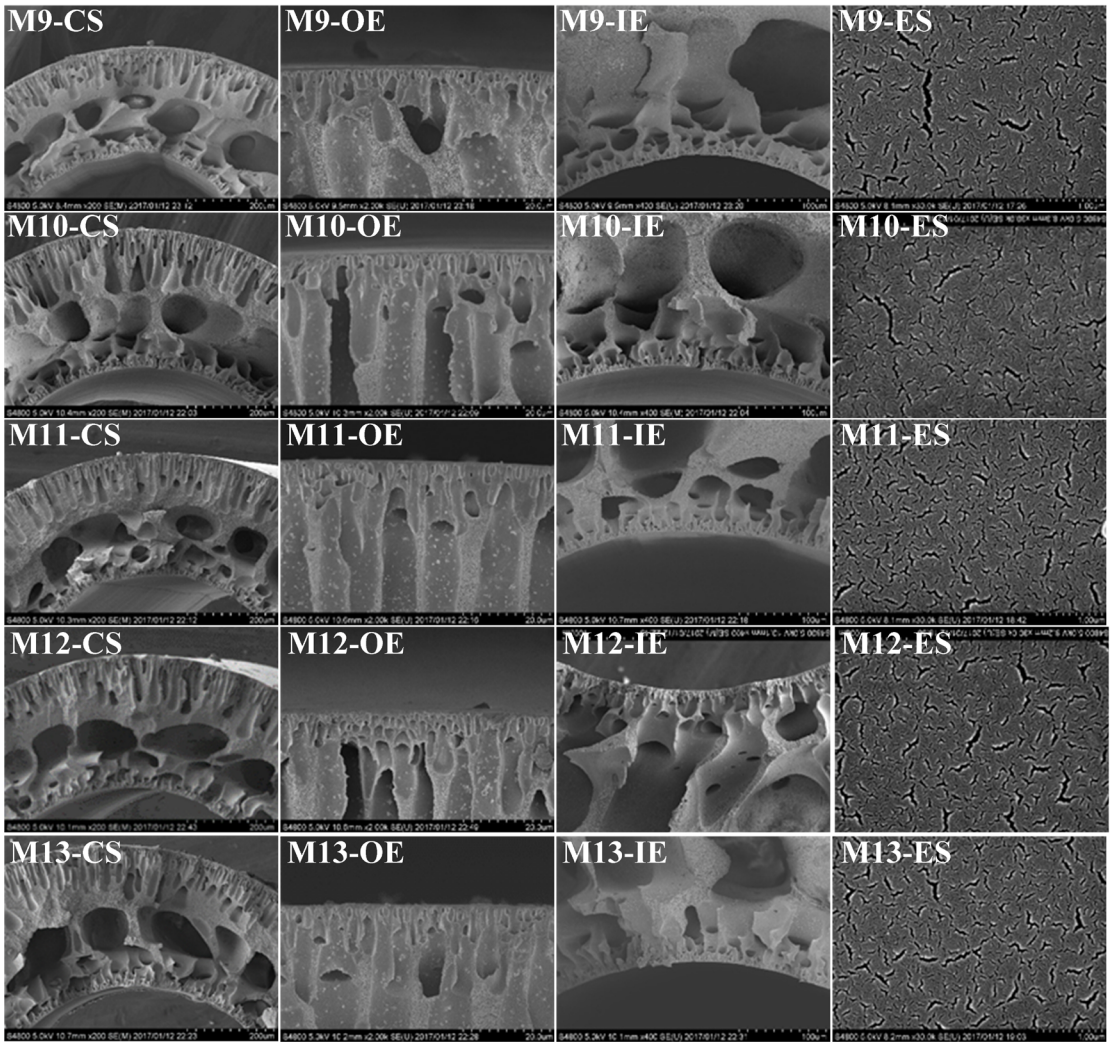

Fig. 7. Effect of PEG content in the polymer solution on the morphologies (CS: cross section; IE: inner edge; OE: outer edge; ES: external surface) of the hollow fiber membranes.

proportion of the PEG chains on the membrane surface penetrate into the membrane pores and are attached on the inner pore surface [38]. In Fig. 7, membrane M0-ES to membrane M10 also show that the external surfaces are denser because the increase of PEG content in the casting solution and water as a coagulation bath, and the dense skin layer is formed due to instantaneous liquid–liquid demixing process [35].

Both porosity and hydrophilicity are important characteristics of ultrafiltration membrane. In order to achieve higher flux, they should be in suitable range. As shown in Table 5, the porosity of membrane with 2wt% PEG as additive was higher than that of the pure PMIA membrane M2 (Fig. 3). This is due to the aqueous solubility of PEG which would result in its leaching out during the membrane fabrication process and lead to a more porous structure [18]. Additionally, membrane M10 (Fig. 8) showed the lowest contact angle at 67.6°, representing good hydrophilicity of the resulting membranes. The hydrophilicity of the PEG doped membrane is also proven by permeate flux tests in which the permeate flux enhanced from 226.85 to 239.63 L $m^2 h^{-1}$ as the PEG concentration increased from 0 to 2wt%, as shown in Fig. 9. Meanwhile, the rejection of BSA increased from 92.90% to 98.50%, implying that the introduction of PEG improved the inter-connectivity and the size of the membrane macropores was suppressed (Table 5). However further increasing the PEG concentration (more than 2wt%) results in the decrease of the permeate flux, this could be due to relatively higher viscosity of the dope in presence of too much PEG. Thus, the exchange rates of solvent and non-solvent would decrease during coagulation process that sponge-like structure occupied the membrane middle section and the porosity of the resulting membranes decreased to some extent.

From Table 5, all the PMIA/LiCl/PEG membranes exhibit the high rejections of above 96.50% for BSA solutes, meanwhile, Fig. 10 presents the membrane pore size are main focus on 10–20 nm, implying good ultrafiltration performances are obtained. To assess filtration efficiency of the membranes, BSA was selected as model foulants in this study. The results are shown in Fig. 11. As shown in Fig. 11, the BSA solution flux of each sample was lower than its pure water flux for the membranes. This is due to the deposition and adsorption of BSA on the surface or due to its entrance into the pores of membrane during filtration under the 1 bar

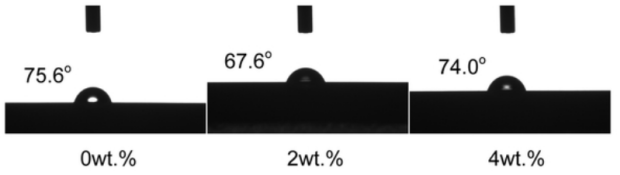

Fig. 8. Contact angle of selected PMIA membrane.

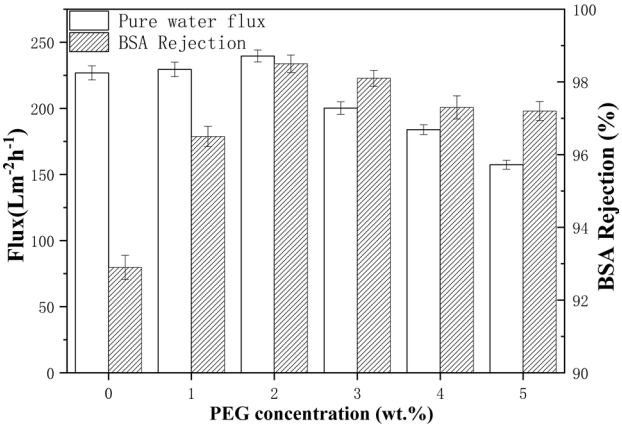

Fig. 9. Effect of PEG concentration on the performance of PMIA hollow fiber UF membranes.

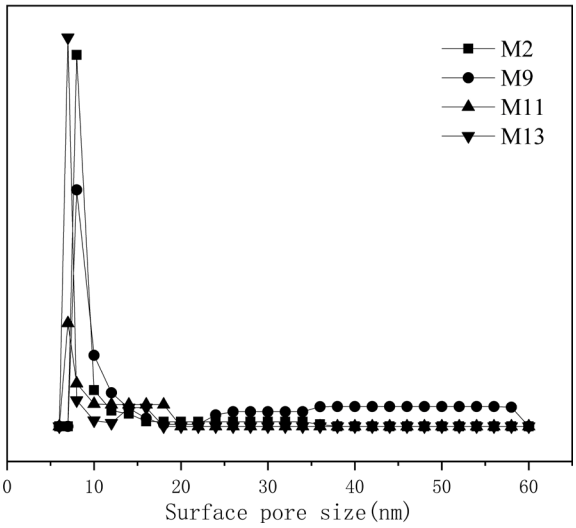

Fig. 10. Pore size distribution of PMIA hollow fiber UF membranes.

Table 5
Effect of PEG concentration on the characteristic of the membrane

Sample	PEG (wt%)	OD (nm)	ID (nm)	δ/mm	Porosity (%)	Mean pore size (nm)	Contact angle (°)	BSA rejection (%)	HA rejection (%)
M2	0	1.221	0.713	0.254	81.17	8.96	74.5 ± 1.8	92.9 ± 0.33	69.9 ± 0.38
M9	1	1.281	0.679	0.301	81.30	9.34	69.7 ± 2.2	96.5 ± 0.28	82.0 ± 0.44
M10	2	1.306	0.728	0.289	81.65	10.28	67.6 ± 1.6	98.5 ± 0.24	90.2 ± 0.63
M11	3	1.304	0.721	0.2915	80.66	9.48	71.4 ± 2.8	98.1 ± 0.22	87.6 ± 0.37
M12	4	1.365	0.722	0.3215	79.22	7.77	74.0 ± 1.4	97.3 ± 0.32	86.9 ± 0.54
M13	5	1.38	0.786	0.297	78.39	7.30	70.3 ± 2.5	97.4 ± 0.26	72.2 ± 0.45

OD, outer diameter, ID, inner diameter, δ, wall thickness.

Table 6
Comparison with other membranes

Dope solution material	Preparation method	Flux (L $m^{-2} h^{-1}$)	Re (%) (BSA, 67,000)	Year	Reference
PS	NIPS	188.5	84.5	2018	[40]
PVDF	Modified	87.8 ± 5.3	94.6 ± 0.4	2017	[41]
Poly(VC-co-PEGMA)/PVC	NIPS	300 ± 10	76 ± 0.2	2017	[42]
PVDF/PFSA/O-MWNTs	NIPS	181.2	96	2016	[43]
PES/$Mg(OH)_2$	NIPS	700 ± 45	90 ± 2.7	2016	[44]
PVDF/WA	NIPS	70.6 ± 5	81 ± 2.1	2016	[45]
PES/p(H-P-A)	NIPS	137 ± 10	57 ± 0.9	2015	[46]
PES/PDMAEMA-b-PES-b-PDMAEMA	NIPS	145 ± 9	70 ± 2.1	2014	[47]
PES/PVDF	TIPS-NIPS	100.7 ± 3.8	80.1	2014	[48]
Present work	NIPS	239.63 ± 9	98.5		

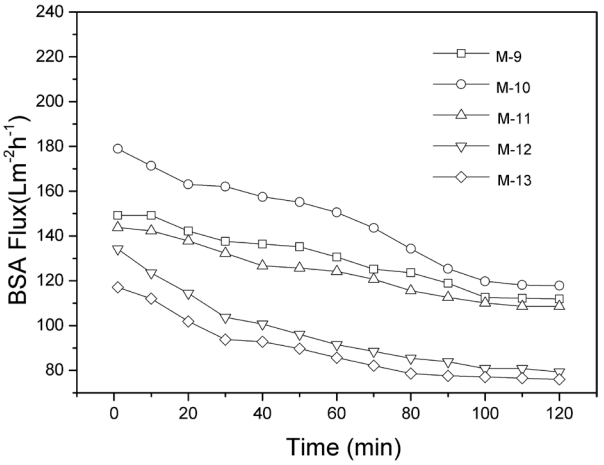

Fig. 11. Flux of the PMIA hollow fiber membranes with 1,000 mg L^{-1} BSA solution.

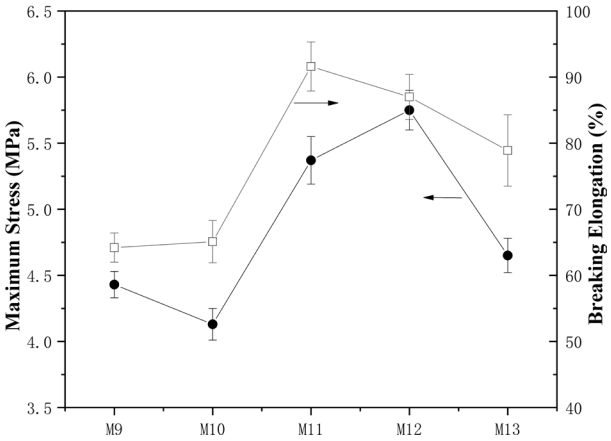

Fig. 12. Breaking elongation and maximum stress of PMIA hollow fiber UF membrane.

feed pressure [39]. The membrane M10 showed the highest flux for BSA solution compared with other samples, because of its high porosity and pore size, lowest contact angle of the membrane surface (Table 5) among all the tested membrane.

3.5. Mechanical properties

The purpose of investigating mechanical performance of the spun fibers is to study the effects of different PEG concentration on the mechanical properties (elongation and maximum stress) of the produced hollow fibers, as shown in Fig. 12. The results indicate that the PEG as an additive had a significant influence on the mechanical properties of the resultant PMIA fibers. By comparing the membranes of M10 with the other prepared membranes, it can be seen from Fig. 12 that the breaking elongation and maximum stress values of the membrane using 2wt% PEG as an additive are correspondingly lower than all the other membranes. This is ascribed to the looser and more porous inner and outer layers of the membrane M10, which is demonstrated in Fig. 7 and Table 5. In addition, the variation of the maximum stress values could be explained by the variation of the membrane wall thickness as explained above (Table 5). However, samples M9-M13 all showed extension values higher than 60% which are able to withstand a water upstream pressure as high as 6 bars. This improvement in extension makes PMIA hollow fiber membrane good candidates for low pressure ultrafiltration processes.

3.6. Comparison with other reported UF membranes

Comparison of flux of the prepared samples was made with other reported UF membrane process in the recent 4 years in this study. Table 6 lists a detailed performance comparison between the present work and the previous investigations. It can be observed that the obtained data in this study is much better than most of the previous reports and comparable with of the best in these reports [41]. Compared with membranes prepared by Zhou et al. [42] and Han et al. [44], the membranes in this work showed lower water flux but higher BSA rejection. Generally speaking, the PMIA hollow fibers ultrafiltration membrane displayed excellent properties on pure water flux, BSA rejection rate.

4. Conclusion

Novel high flux PMIA hollow fiber ultrafiltration membranes were successfully fabricated by the dry/wet phase inversion technique in this study and the results show a

significant improvement of pure water flux and rejection of BSA. The increase of PMIA content and LiCl concentration in the dope solution could change the morphologies of UF membranes from loose macrovoids into more favorable finger-like and sponge-like structures. The addition of PEG in casting solution endows the membrane with higher hydrophilicity, porosity which improves permeability and rejection rate of BSA a lot. Results showed that membrane under optimized conditions (LiCl 4wt%, PEG 2wt%) exhibited the highest pure water flux (239.63 L $m^{-2} h^{-1}$) and highest rejection rate of BSA (98.50%) under the operation pressure of 0.1 Mpa in this study. Moreover, the newly prepared PMIA hollow fiber UF membranes exhibited excellent mechanical strength and have great potential for practical application in wastewater filtration.

Conflicts of interest

There are no conflicts to declare.

Acknowledgments

This work was supported through the grants from the Bureau Frontier Sciences and Education (QYZDB-SSW-DQC044), the Bureau of International Cooperation (132C35KYSB20160018), Chinese Academy of Sciences and the Joint Project between CAS-CSIRO. The authors would like to thank the reviewers and Dr. Olusegun Abass for their useful comments, help and assistance.

References

[1] G. Daufin, J.P. Escudier, H. Carrere, S. Berot, L. Fillaudeau, M. Decloux, Recent and emerging applications of membrane processes in the food and dairy industry, Food. Bioprod. Process, 79 (2001) 89–102.
[2] W. Gao, H. Liang, J. Ma, M. Han, Z.L. Chen, Z.S. Han, G.B. Li, Membrane fouling control in ultrafiltration technology for drinking water production: a review, Desalination, 272 (2011) 1–8.
[3] J. Zhang, M.Y. Zhang, K.S. Zhang, Fabrication of poly(ether sulfone)/poly(zinc acrylate) ultrafiltration membrane with anti-biofouling properties, J. Membr. Sci., 460 (2014) 18–24.
[4] H. Okuno, K. Renzo, T. Uragami, Influence of casting solution additive, degree of polymerization, and polymer concentration on poly(vinyl chloride) membrane-properties and performance, J. Membr. Sci., 83 (1993) 199–209.
[5] B.C. Liu, C. Chen, W. Zhang, J. Crittenden, Y.S. Chen, Low-cost antifouling PVC ultrafiltration membrane fabrication with Pluronic F 127: effect of additives on properties and performance, Desalination, 307 (2012) 26–33.
[6] E. Villaverde-de-Saa, I. Racamonde, J.B. Quintana, R. Rodil, R. Cela, Ion-pair sorptive extraction of perfluorinated compounds from water with low-cost polymeric materials: polyethersulfone vs polydimethylsiloxane, Anal. Chim. Acta, 740 (2012) 50–57.
[7] G.D. Kang, Y.M. Cao, Application and modification of poly(vinylidene fluoride) (PVDF) membranes - a review, J. Membr. Sci., 463 (2014) 145–165.
[8] M.Y. Zhang, K.S. Zhang, B. De Gusseme, W. Verstraete, Biogenic silver nanoparticles (bio-Ag-0) decrease biofouling of bio-Ag-0/PES nanocomposite membranes, Water Res., 46 (2012) 2077–2087.
[9] F. Liu, N.A. Hashim, Y.T. Liu, M.R.M. Abed, K. Li, Progress in the production and modification of PVDF membranes, J. Membr. Sci., 375 (2011) 1–27.
[10] Y. Zheng, W. Zhang, B. Tang, J. Ding, Y. Zheng, Z. Zhang, Membrane fouling mechanism of biofilm-membrane bioreactor (BF-MBR): pore blocking model and membrane cleaning, Bioresour. Technol., 250 (2018) 398–405.
[11] B. Wang, K.S. Zhang, R.W. Field, Slug bubbling in flat sheet MBRs: hydrodynamic optimization of membrane design variables through computational and experimental studies, J. Membr. Sci., 548 (2018) 165–175.
[12] X. Wu, Z.L. Xie, H.T. Wang, C. Zhao, D. Ng, K.S. Zhang, Improved filtration performance and antifouling properties of polyethersulfone ultrafiltration membranes by blending with carboxylic acid functionalized polysulfone, RSC Adv., 8 (2018) 7774–7784.
[13] P. Nimmanpipug, K. Tashiro, O. Rangsiman, Factors governing the three-dimensional hydrogen-bond network structure of poly(m-phenylene isophthalamide) and a series of its model compounds (4): similarity in local conformation and packing structure between a complicated three-arm model compound and the linear model compounds, J. Phys. Chem. B, 110 (2006) 20858–20864.
[14] M.X. Chen, C.F. Xiao, C. Wang, H.L. Liu, Study on the structural design and performance of novel braid-reinforced and thermostable poly(m-phenylene isophthalamide) hollow fiber membranes, RSC Adv., 7 (2017) 20327–20335.
[15] A.V. Bildyukevich, T.V. Plisko, A.S. Liubimova, V.V. Volkov, V.V. Ususky, Hydrophilization of polysulfone hollow fiber membranes via addition of polyvinylpyrrolidone to the bore fluid, J. Membr. Sci., 524 (2017) 537–549.
[16] J. Han, D. Yang, S. Zhang, X. Jian, Effects of dope compositions on the structure and performance of PPES hollow fiber ultrafiltration membranes, J. Membr. Sci., 345 (2009) 257–266.
[17] D. Hua, S. Japip, K.Y. Wang, T.S. Chung, Green design of poly(m-phenylene isophthalamide)-based thin-film composite membranes for organic solvent nanofiltration and concentrating lecithin in hexane, ACS Sustain. Chem. Eng., 6 (2018) 10696–10705.
[18] J. Huang, K. Zhang, The high flux poly (m-phenylene isophthalamide) nanofiltration membrane for dye purification and desalination, Desalination, 282 (2011) 19–26.
[19] T. Wang, C. Zhao, P. Li, Y. Li, J. Wang, Effect of non-solvent additives on the morphology and separation performance of poly(m-phenylene isophthalamide) (PMIA) hollow fiber nanofiltration membrane, Desalination, 365 (2015) 293–307.
[20] M. Chen, C. Xiao, C. Wang, H. Liu, N. Huang, Preparation and characterization of a novel thermally stable thin film composite nanofiltration membrane with poly (m-phenyleneisophthalamide) (PMIA) substrate, J. Membr. Sci., 550 (2018) 36–44.
[21] Q. Luo, Y. Liu, G. Liu, C. Zhao, Preparation, characterization and performance of poly(m-phenylene isophthalamide)/organically modified montmorillonite nanocomposite membranes in removal of perfluorooctane sulfonate, J. Environ. Sci. China, 46 (2016) 126–133.
[22] M. Yang, C. Zhao, S. Zhang, P. Li, D. Hou, Preparation of graphene oxide modified poly(m-phenylene isophthalamide) nanofiltration membrane with improved water flux and antifouling property, Appl. Surf. Sci., 394 (2017) 149–159.
[23] T.S. Chung, E.R. Kafchinski, The effects of spinning conditions on asymmetric 6FDA/6FDAM polyimide hollow fibers for air separation, J. Appl. Polym. Sci., 65 (1997) 1555–1569.
[24] Y. Yang, D. Yang, S. Zhang, J. Wang, X. Jian, Preparation and characterization of poly(phthalazinone ether sulfone ketone) hollow fiber ultrafiltration membranes with excellent thermal stability, J. Membr. Sci., 280 (2006) 957–968.
[25] W.-Z. Lang, J.-P. Shen, Y.-X. Zhang, Y.-H. Yu, Y.-J. Guo, C.-X. Liu, Preparation and characterizations of charged poly(vinyl butyral) hollow fiber ultrafiltration membranes with perfluorosulfonic acid as additive, J. Membr. Sci., 430 (2013) 1–10.
[26] P. Liu, S. Zhang, Y. Wang, Y. Lu, X. Jian, Preparation and characterization of thermally stable copoly(phthalazinone biphenyl ether sulfone) hollow fiber ultrafiltration membranes, Appl. Surf. Sci., 335 (2015) 189–197.

[27] H.A. Tsai, M.J. Hong, G.S. Huang, Y.C. Wang, C.L. Li, K.R. Lee, J.Y. Lai, Effect of DGDE additive on the morphology and pervaporation performances of asymmetric PSf hollow fiber membranes, J. Membr. Sci., 208 (2002) 233–245.
[28] X. Kong, M.Y. Zhou, C.E. Lin, J. Wang, B. Zhao, X.Z. Wei, B.K. Zhu, Polyamide/PVC based composite hollow fiber nanofiltration membranes: effect of substrate on properties and performance, J. Membr. Sci., 505 (2016) 231–240.
[29] R.I. Peinador, J.I. Calvo, P. Pradanos, L. Palacio, A. Hernandez, Characterisation of polymeric UF membranes by liquid-liquid displacement porosimetry, J. Membr. Sci., 348 (2010) 238–244.
[30] H.L. Liu, C.F. Xiao, X.Y. Hu, M.T. Liu, Post-treatment effect on morphology and performance of polyurethane-based hollow fiber membranes through melt-spinning method, J. Membr. Sci., 427 (2013) 326–335.
[31] L.Y. Yu, Z.L. Xu, H.M. Shen, H. Yang, Preparation and characterization of PVDF-SiO_2 composite hollow fiber UF membrane by sol-gel method, J. Membr. Sci., 337 (2009) 257–265.
[32] F. Tasselli, J.C. Jansen, E. Drioli, PEEKWC ultrafiltration hollow-fiber membranes: preparation, morphology, and transport properties, J. Appl. Polym. Sci., 91 (2004) 841–853.
[33] I.C. Kim, K.H. Lee, T.M. Tak, Preparation and characterization of integrally skinned uncharged polyetherimide asymmetric nanofiltration membrane, J. Membr. Sci., 183 (2001) 235–247.
[34] R.E. Kesting, Semipermeable membranes of cellulose acetate for desalination in process of reverse osmosis. I. Lyotropic swelling of secondary cellulose acetate, J. Appl. Polym. Sci., 9 (1965) 663–688.
[35] B. Jung, J.K. Yoon, B. Kim, H.W. Rhee, Effect of molecular weight of polymeric additives on formation, permeation properties and hypochlorite treatment of asymmetric polyacrylonitrile membranes, J. Membr. Sci., 243 (2004) 45–57.
[36] J.A. Prince, S. Bhuvana, K.V.K. Boodhoo, V. Anbharasi, G. Singh, Synthesis and characterization of PEG-Ag immobilized PES hollow fiber ultrafiltration membranes with long lasting antifouling properties, J. Membr. Sci., 454 (2014) 538–548.
[37] L.B. Zheng, Z.J. Wu, Y.S. Wei, Y. Zhang, Y. Yuan, J. Wang, Preparation of PVDF-CTFE hydrophobic membranes for MD application: effect of LiCl-based mixed additives, J. Membr. Sci., 506 (2016) 71–85.
[38] W.L. Chou, D.G. Yu, M.C. Yang, C.H. Jou, Effect of molecular weight and concentration of PEG additives on morphology and permeation performance of cellulose acetate hollow fibers, Sep. Purif. Technol., 57 (2007) 209–219.
[39] M. Hashino, K. Hirami, T. Katagiri, N. Kubota, Y. Ohmukai, T. Ishigami, T. Maruyama, H. Matsuyama, Effects of three natural organic matter types on cellulose acetate butyrate microfiltration membrane fouling, J. Membr. Sci., 379 (2011) 233–238.
[40] A. Khan, T.A. Sherazi, Y. Khan, S. Li, S.A.R. Naqvi, Z. Cui, Fabrication and characterization of polysulfone/modified nanocarbon black composite antifouling ultrafiltration membranes, J. Membr. Sci., 554 (2018) 71–82.
[41] W. Miao, Z.-K. Li, X. Yan, Y.-J. Guo, W.-Z. Lang, Improved ultrafiltration performance and chlorine resistance of PVDF hollow fiber membranes via doping with sulfonated graphene oxide, Chem. Eng. J., 317 (2017) 901–912.
[42] Z. Zhou, S. Rajabzadeh, L. Fang, T. Miyoshi, Y. Kakihana, H. Matsuyama, Preparation of robust braid-reinforced poly(vinyl chloride) ultrafiltration hollow fiber membrane with antifouling surface and application to filtration of activated sludge solution, Mater. Sci. Eng. C, 77 (2017) 662–671.
[43] X. Zhang, W.-Z. Lang, X. Yan, Z.-Y. Lou, X.-F. Chen, Influences of the structure parameters of multi-walled carbon nanotubes(MWNTs) on PVDF/PFSA/O-MWNTs hollow fiber ultrafiltration membranes, J. Mater. Sci., 499 (2016) 179–190.
[44] S.J. Han, L.L. Mao, T. Wu, H.Z. Wang, Homogeneous polyethersulfone hybrid membranes prepared with in-situ synthesized magnesium hydroxide nanoparticles by phase inversion method, J. Mater. Sci., 516 (2016) 47–55.
[45] X.Z. Zhao, C.K. Liu, One-step fabricated bionic PVDF ultrafiltration membranes exhibiting innovative antifouling ability to the cake fouling, J. Mater. Sci., 515 (2016) 29–35.
[46] X.L. Zhan, G.F. Zhang, X. Chen, R. He, Q.H. Zhang, F.Q. Chen, Improvement of antifouling and antibacterial properties of poly(ether sulfone) UF membrane by blending with a multifunctional comb copolymer, Ind. Eng. Chem. Res., 54 (2015) 11312–11318.
[47] A.W. Qin, X.L. Wu, B.M. Ma, X.Z. Zhao, C.J. He, Enhancing the antifouling property of poly(vinylidene fluoride)/SiO_2 hybrid membrane through TIPS method, J. Mater. Sci., 49 (2014) 7797–7808.
[48] T.-Y. Liu, R.-X. Zhang, Q. Li, B. Van der Bruggen, X.-L. Wang, Fabrication of a novel dual-layer (PES/PVDF) hollow fiber ultrafiltration membrane for wastewater treatment, J. Membr. Sci., 472 (2014) 119–132.